Development 128, 3819-3830 (2001)
Printed in Great Britain © The Company of Biologists Limited 2001
DEV3484

Cell survival and proliferation are modified by insulin-like growth factor 2 between days 9 and 10 of mouse gestation

Jason L. Burns and A. Bassim Hassan*

Department of Zoology, University of Oxford, South Parks Road, Oxford OX1 3PS, UK
*Author for correspondence (e-mail: bass.hassan@zoo.ox.ac.uk)

Accepted 5 July 2001

SUMMARY

The size of mammalian species involves the interaction of multiple genetic modifiers that control the timing and extent of growth mechanisms. Disruption of the paternal allele of the imprinted embryonic gene coding for insulin-like growth factor 2 (IGF2, *Igf2*$^{+m/-p}$), results in viable mice that are 60% the weight of wild-type littermates. Differences in weight are first detected at embryonic day (E) 11, and the growth deficit is maintained throughout life. We report the mechanisms that account for this unusual phenotype. In order to quantify growth, we used novel methods to generate single cell suspensions of post-implantation mouse embryos. We were then able to quantify cell number, cell proliferation and cell death between E8.5 and E11.5 using flow cytometry. Determination of total embryo cell number also allowed us to time litters by a method other than by plugging. Wild-type and *Igf2*$^{+m/-p}$ embryos accumulated similar total cell numbers up to E9.25, but cell number began to diverge by around E9.5, with significant differences by E11 (75% of wild type). A relative increase in pyknotic nuclei, sub-G1 cytometry counts and caspase activity, all indicative of cell death, occurred in *Igf2*$^{+m/-p}$ embryos at E9.25, reverting to wild-type levels by E9.75. This was followed at E9.75 by a significant reduction in the proportion of cells in S phase, quantified by S-phase cytometry counts and BrdU labelling. No significant differences in cell size were detected. We conclude that the majority of the cell number differences between wild-type and *Igf2*$^{+m/-p}$ mice can be accounted for by modification of cell survival and proliferation during the period (E9 to E10) of post-implantation development.

Key words: Insulin-like growth factor 2, Embryo cell number, Cell survival, Cell proliferation, Embryonic growth, Mouse

INTRODUCTION

The control of growth requires a complex set of interactions operating at systemic, cellular and molecular levels, which ultimately determine the size of a cell, tissue, organ or organism. The co-ordination of cell growth (mass), cell number (proliferation), cell death (apoptosis) and differentiation is particularly important in relation to location and time during development (Conlon and Raff, 1999; Weinkove et al., 1999). In mammalian species, nutrient supply, hormones and growth factors are the principal determinants of whole organism cell number. Growth hormone (GH), insulin-like growth factor 1 (IGF1), Insulin-like growth factor 2 (IGF2) and their receptors, growth hormone receptor (GHr), insulin-like growth factor 1 receptor (IGF1R) and insulin-like growth factor 2/mannose 6-phosphate receptor (IGF2R) have been shown to modify the growth of mice following disruption of respective genes (Efstratiadis, 1998; Louvi et al., 1997; Ludwig et al., 1996; Lupu et al., 2001). Disruption of the *Igf2* gene results in a fertile mouse with almost half the adult body weight but apparently normal proportions (DeChiara et al., 1990; DeChiara et al., 1991). Disruption of IGF1 (*IgfI*$^{-/-}$) results in embryonic growth retardation detectable from E12.5-E13.5 (60% of wild type), but unlike *Igf2*$^{-/-}$, the growth rate continues to decline postnatally (to 30% of wild type) (Liu et al., 1993). Genetic crosses between these mice and *Igf1r*$^{-/-}$, have established that IGF1R produces IGF2-mediated embryonic growth at least between E11.0 to E13.5, and IGF1-mediated growth thereafter to postnatal day 40 (Baker et al., 1993; Lupu et al., 2001). However normal embryonic growth in *Igf2r*$^{-/-}$, *Igf1r*$^{-/-}$ mice suggests that the increased IGF2 supply after disruption of *Igf2r*$^{-/-}$ is mediated by an alternative receptor, which is probably the insulin receptor (Ir) (Louvi et al., 1997; Ludwig et al., 1996). Although IGF1 endocrine supply may be affected by the action of GH on the liver, it appears that GH acts both with IGF1-dependent and -independent activity during postnatal growth (Lupu et al., 2001). The only similar growth phenotype to *Igf2* disruption occurs after disruption of insulin receptor substrate 1 (IRS1). *Irs1*$^{-/-}$ are born 40-60% smaller than wild-type littermates and maintain this proportionate size difference throughout life; they have normal bone development, are fertile and have normal litter sizes (Araki et al., 1994).

Another unusual feature following disruption of *Igf2* is the observation that the same growth phenotype follows either homozygous disruption (–m/–p) or disruption of the paternal

Igf2 allele alone (+m/–p). This effect is due to genomic imprinting, which normally results in silencing of gene expression from the maternal allele (DeChiara et al., 1991; Tilghman, 1999). Although using PCR there is evidence of *Igf2* expression during pre-implantation development, in situ hybridisation first localises *Igf2* mRNA in the extra-embryonic ectoderm and ecto-placental cone during early implantation (E5.5; Lee et al., 1990). Expression then concentrates around extra-embryonic mesoderm emerging from, but not including, the primitive streak, as well as columnar visceral endoderm (E7). It is not until E7.5 that mRNA can be visualised clearly in the embryo proper, initially in embryonic mesoderm, then lateral mesoderm and the developing heart, foregut and somites (E7.5-E8.5; Lee et al., 1990). Despite early expression in tissues that form the chorioallantoic placenta, the weight of the placenta remains the same in wild type and *Igf2*$^{+m/-p}$ until E13.5 (Baker et al., 1993). The distribution of pre-pro IGF2 and IGF2R matches that of *Igf2* mRNA and suggests that IGF2 supply arises mainly from mesoderm (Morali et al., 2000; Senior et al., 1990). Furthermore, these observations suggest that the growth defect following genetic disruption of the *Igf2* gene occur later than the detection of mRNA expression. Although the reason for this is unknown, potential explanations include alterations in mRNA half-life, mRNA translation, storage and release of IGF2 protein, and modification of the location and extent of IGF2 extra-cellular protein supply, which may also affect downstream growth control genes (e.g. *p57* ^{kip2}; Grandjean et al., 2000; Nielson et al., 1999; Van der Velden et al., 2000).

IGF2 can act as a cell survival factor, mitogenic factor and can also modify metabolism (Da Costa et al., 1994; Lee et al., 1990; Lopez et al., 1996). The IGF system, including ligand structure and receptors, appears evolutionary conserved. For example, recent genetic studies in *Drosophila* have confirmed the essential role of the insulin-like growth factor system in controlling organ, body and cell size (Bohni et al., 1999; Brogiolo et al., 2001; Goberdhan et al., 1999; Weinkove et al., 1999). Multiple downstream pathways, such as IRS1, IRS2, Akt, Bad, PI3-kinase, cyclin D1 and Ras, are modulated after IGF1R-ligand interaction (Datta et al., 1997; Downward, 1998). Disruption of the genes encoding these proteins can also result in embryonic growth phenotypes in mouse (Araki et al., 1994; Bi et al., 1999; Sicinski et al., 1995).

Overexpression of IGF2 occurs commonly in tumours, and can result in the foetal overgrowth syndromes (Christofori et al., 1995; Eggenschwiler et al., 1997; Hassan and Howell, 2000; Sun et al., 1997). Increased supply of embryonic IGF2 frequently results in disproportionate overgrowth associated with heart enlargement, oedema and foetal death, and may account for large offspring syndrome after nuclear transfer and in vitro culture (Lau et al., 1994; Sun et al., 1997; Young et al., 2001). Overgrowth after increased IGF2 supply is not always lethal. If it occurs after biallelic *Igf2* gene expression, specifically after disruption of *H19* that includes an upstream boundary element, a fertile and viable mouse is obtained that can completely rescue the growth deficiency of *Igf*$^{+m/-p}$ (Leighton et al., 1995; Srivastava et al., 2000). The magnitude and reproducibility of these observations suggest that the growth effects of IGF2 are developmentally programmed. This led us to consider that the normal timing, location and duration of IGF2 supply may be crucially important.

In order to investigate the mechanism of IGF2 embryonic growth control in vivo, we required methods that improve on weight and morphometry alone as measures of growth. We applied methods that generate cell suspensions of whole embryos in order to count cells, as had been developed in *Drosophila* embryos (Krasnow et al., 1991). Using the rapid and accurate method of flow cytometry, we were able to quantify cell number, cell size, cell proliferation and caspase-mediated cell death between days 8.5 to 11.5 of mouse post-implantation development. Our results suggest that the cell death and proliferation detectable during mouse embryogenesis are significantly modified by genetic disruption of IGF2 between E9-E10. Both decreased cell survival and proliferation may be the mechanisms that account for a significant proportion of the differences in growth of *Igf2*$^{+m/-p}$ in *Mus musculus* (*129/SvJ*). The timing and duration of this effect may subsequently be important for size control in other mammalian species.

MATERIALS AND METHODS

Foetal examination

*Igf*2$^{+m/-p}$ male mice (inbred*129/SvJ)* were mated with wild-type females and housed under a 12 hour light (6 am to 6 pm)/12 hour dark cycle. *Igf*2$^{+m/-p}$ were used as the phenotype matches for *Igf*2$^{-m/-p}$. Convention dictates that the day of plug detection equates to embryonic day 0.5 (E0.5). However, in our case, inspection for seminal plugs were performed at 9 am and 5 pm, with the midpoint times, 1 am and 1 pm, respectively, taken as the times of conception. The embryonic age (in days) was calculated by dividing the total number of hours between plug time (either 1 am or 1 pm) and the time of embryonic dissection, by 24. Using this method for daytime plugs, embryonic age would vary on average by ±4 hours (0.18 days) and, for night-time plugs, by ±8 hours (0.33 days). This method allowed us to rank multiple litters previously timed together at a specific time (e.g. E9.5), to times slightly before or slightly after. Initially, we tried 2-4 hour periods of mating to increase the accuracy of conception time but this provided us with too few plugs.

Embryos were dissected from placental membranes in ice-cold Ca^{2+} and Mg^{2+} free phosphate-buffered saline (PBS) and, depending on the assay, either fixed in ice-cold ethanol:glacial acetic acid (3:1, analytical grade) and stored at 4°C (24 hours minimum), or were fixed in 4% (w/v) paraformaldehyde (Sigma) in filtered PBS (pH 7.4) for 24 hours followed by 70% ethanol, or embedded for frozen sections in OCT (Sakura Fintek, Netherlands, 7 μm cryo-sections). Dissections of each litter normally took no longer than 20 minutes, from removal of uterine horns to embryo fixation. Extra-embryonic membranes were used for PCR analysis (Zaina and Squire, 1998). Somites and morphological features were examined using transmitted light examination of fixed whole embryos (×50). All animal procedures were approved by the UK Home Office and local ethics committee.

In situ analysis of embryos

Unfixed whole embryos were immediately examined for pyknotic nuclei using Acridine Orange (AO) and confocal microscopy (Abrams et al., 1993). After incubation (AO 100 ng/ml in modified Eagle's medium (MEM), 30 minutes, 4°C) and washing (PBS, 5 minutes), embryos were examined using an MRC Confocal Microscope 1024 (14MW Argon laser, 594 nm) with a ×10 Nikon objective. TUNEL assays (Oncor kit and Roche reagents) were performed on frozen cryo-sections placed on adhesive treated slides (3-aminopropyl-triethoxy-silane), fixed with 4% (w/v) paraformaldehyde in PBS (pH 7.4, at 4°C, 5 minutes) followed by washing in graded ethanol series before air drying. Slides were then re-hydrated in PBS, endogenous peroxidases quenched with 3% H_2O_2 and TUNEL protocol, according

to the manufacturer's instructions. Slides were counter-stained with Methyl Green (1% v/v distilled H_2O). Incorporated digoxigenin dUTP (Roche) was detected with an anti-digoxigenin Fab fragment peroxidase. Positive controls were performed with each assay batch and included either cryo-sections from adult mouse testis, mammary glands during involution and DNaseI (1000 U/ml in 30mM Tris-HCl, pH 7.4, 50mM NaCl, 5mM $MgCl_2$ for 5 minutes at room temperature (Sigma)) -treated embryo sections. DNAseI-treated samples were also assayed without the addition of either terminal transferase (tdt) or digoxigenin-conjugated dUTP. Two sections were typically applied to each slide, with only one being exposed to the reaction mixture, the other used as a control with the absence of either tdt or digoxigenin-dUTP to measure nonspecific labelling.

BrdU (Sigma) incorporation was detected after a single intra-peritoneal injection (100 μg/g body weight; Bi et al., 1999). After fixation, sections were incubated with 1.5 M HCl for 15 minutes to acid denature the DNA. After washes (twice in cold PBS, 0.05% bovine serum albumin (BSA) and 0.01% Tween 20), sections were incubated with anti-BrdU-antibody conjugated with FITC at 37°C for 30 minutes in the dark (1/5 dilution, Roche). Samples were washed (twice in cold PBS), counterstained with 0.02% Fast Green, washed again (twice) and viewed with an Olympus fluorescent microscope (BX60). Controls included embryos from wild-type females not injected with BrdU.

Embryonic cell suspensions and cytometry

Several different methods of generating single cell suspensions were attempted. Although single cell suspensions could be generated from unfixed material, we preferred fixation to facilitate the analysis of large numbers of embryos. Addition of either collagenase or proteases were not required for embryos between E8.8 and E11.4, but were necessary for embryos at E12.5 because of significant aggregation. Single cell suspensions were produced by placing fixed embryos (3:1 ethanol:glacial acetic acid), into 60% (v/v) glacial acetic acid in sterile filtered distilled H_2O for 30 minutes at room temperature. This was followed by gentle pipetting using a 1000 μl plastic tip, dissociating the embryo into a cell suspension. To inspect suspensions, droplet spreads were made on ethanol-washed glass slides dried using compressed air to remove dust particles. Spreads were dried at room temperature, stained with DAPI (1 μg/ml) in Citifluor (Agar) and viewed with a fluorescent microscope and CCD camera (Olympus). Digital images were examined using NIH image (1.6.1) and mitotic figures and pyknotic nuclei could be counted. Total nuclear fluorescence was determined by drawing around each nucleus and determining the integrated fluorescence density. Cell suspensions were routinely checked for aggregates and counted with a haemocytometer. For accurate cell counts, and to measure DNA content profiles, aliquots of cell suspensions were examined by flow cytometry. Here, cell suspensions in 60% glacial acetic acid were spun at 500 ***g*** for 10 minutes, washed once with cold PBS, spun at 500 ***g*** for 10 minutes, re-suspended in propidium iodide (50 μg/ml) and RNAse A (100 μg/ml) in PBS (37°C, sterile 0.2μm filtered, 30 minutes in dark) before analysis with a Coulter EPICS/XL cytometer and associated software. From 1000 μl total suspension, 100 μl was routinely counted per embryo, whether wild type or *Igf2*$^{+m/-p}$, and was used to calculate total cell number and cell number subtracting the sub-G1 component. A minimum of 10,000 events were collected from each embryo for cell counts and DNA content profiles (see Results). In order to exclude interference from either embryo or non-embryo debris, controls performed in each batch included cells in PBS only, and solutions of propidium iodide (50 μg/ml) and RNAse A (100 μg/ml) in PBS without cells, in order to exclude nonspecific particle counts. Serial dilution of cell suspensions and repeated counts of the same suspension were reproducible (R=0.99).

For flow cytometric analysis of BrdU incorporation, embryo suspensions in 60% glacial acetic acid were spun at 500 ***g*** for 10 minutes, re-suspended in pyrex glass tubes (5 ml) and incubated in 1.5M HCl for 15 minutes at room temperature to acid denature DNA. After washes in buffer (twice in cold PBS, 0.05% BSA and 0.01% Tween 20), cells were incubated with mouse anti-BrdU (1/50, Becton Dickinson) in wash buffer for 45 minutes at room temperature. After washes (twice in cold PBS), cells were incubated with goat anti-mouse-FITC (1/10, Becton Dickinson) in wash buffer for a further 45 minutes. Cells were then washed (twice in cold PBS) and re-suspended in PBS with propidium iodide (10 μg/ml) and RNAse A (100 μg/ml) (37°C, 30 minutes in the dark) before dual colour flow cytometry. Controls included solutions without cells, as above, and primary and secondary antibodies alone, with and without propidium iodide to eliminate bleed through. For detection of serine 10 α-phosphorylation of histone H3, a rabbit polyclonal primary antibody (a gift from L. Mahadevan) was used with biotinylated anti-rabbit secondary antibody (1/200, Vector) followed by FITC-streptavidin (1/1000, Sigma).

Cell size analysis and caspase activity

For both analysis, unfixed cell suspensions were generated. Immediately after removal from the uterus, unfixed embryos were converted into cell suspensions by gentle dissociation through a 35 μm nylon filter (Becton Dickinson) in ice-cold MEM without additions. Between E8.8 and E11.4, embryos were rapidly dissociated by the use of a blunt tip (e.g. a microfuge tube) in a slow circular movement around the filter. Filters were flushed using MEM (5 ml) to remove cells, and were then inspected using a phase contrast microscope to ensure complete clearance of cells from the lattice. This procedure was adapted from standard procedures used to generate thymocyte suspensions (Tough and Sprent, 1994). For cell size analysis, unfixed suspensions were examined by a Coulter Multisizer and cell diameter measurements calibrated with 9.7 μm beads (Coulter). Cell concentrations were 5×10^4 cells per ml, and a minimum of 3×10^4 cells were analysed. Red blood cells peaked at (~4 μm). For caspase activity, unfixed suspensions were spun at 500 ***g*** (10 minutes), re-suspended in MEM and incubated (37°C, 1 hour in the dark) with the fluorescence labelled caspase inhibitor, benzyloxycarbonyl valylalanyl aspartic acid-fluoromethyl ketone (FAM-VAD-FMK, Intergen). Cells were washed, gently re-suspended in MEM and propidium iodide (1.25 μg/ml) and analysed immediately with dual colour flow cytometry. Controls included cells with propidium iodide (1.25 μg/ml) or FAM-VAD-FMK alone to determine background levels from signal.

DNA content

DNA content was determined using Hoechst 33258 method with modification (Labarca and Paigen, 1980). Embryos were frozen in liquid nitrogen immediately after removal from the uterus and stored at –80°C. After thawing on ice, embryos were homogenised in 1 ml buffer (50 mM Tris-HCl, 10 mM EDTA, 150 mM NaCl and 0.01% Triton X-100) followed by sonication (10 seconds). Aliquots of crude extract were diluted depending of the size of embryo, and incubated with Hoechst 33258 (0.5 μg/ml in 2 M NaCl, 0.01% Triton X-100, 100 μg/ml RNAse A at room temperature for 15 minutes). Standard curves were generated from serial dilutions of calf thymus DNA (0.5 μg/ml to 32 μg/ml) and samples were read using a Wallac fluorometer (at 460 nm). A buffer control was used to determine background.

Minitab10Xtra was used for all statistical analysis with Student's *t*-test (95% CI), box plots and curve fitting.

RESULTS

In situ localisation of cell proliferation and cell death

Comparison of littermate wild-type and *Igf2*$^{+m/-p}$ mice at E16 and postnatal day (P) 1 revealed a 20% reduction in total DNA content, a ratio that is similar to the ratio of cell number at E11

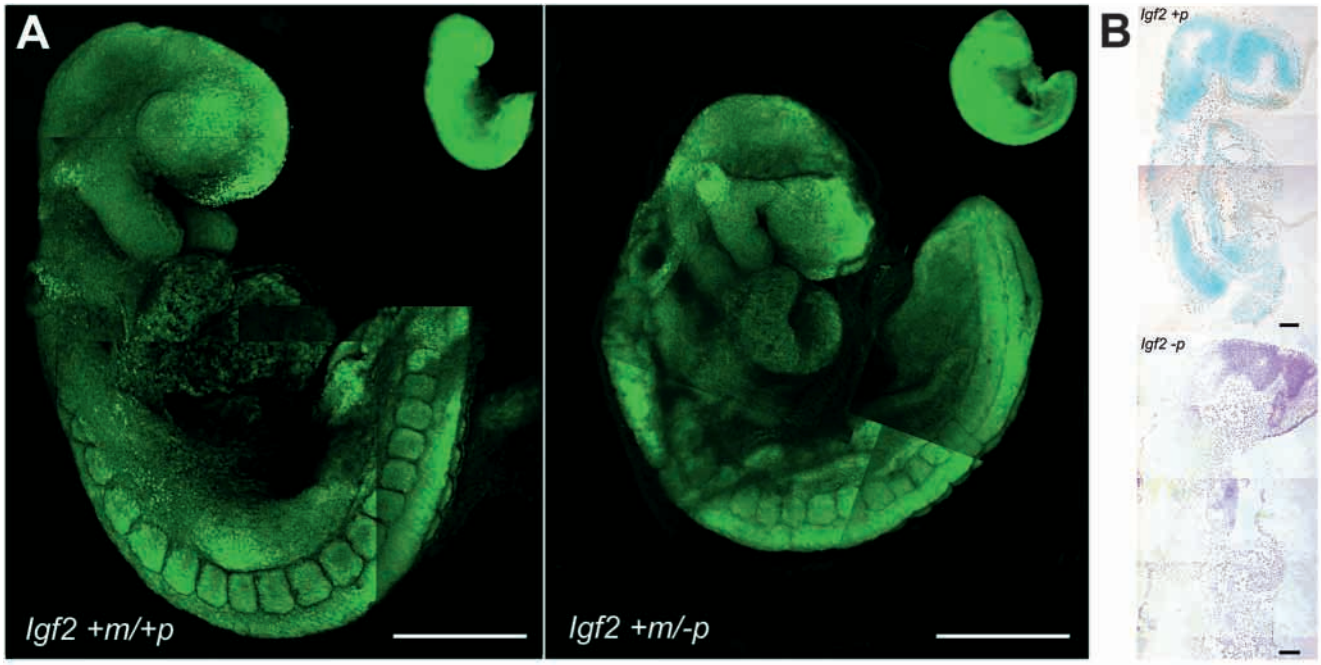

Fig. 1. In situ analysis of cell death E9-E9.5. (A) Acridine Orange staining of pyknotic cells in unfixed embryos (19 somites). Conventional fluorescence microscopy (inserts) at low power reveal similar sized and stained embryos, despite differences in folding and angles of view (left panel, wild type=*Igf2*$^{+m/+p}$; right panel *Igf2*$^{+m/-p}$). Confocal microscopy and maximum projection of the same embryos (18×~5μm sections at 20 μm intervals, large images) reveal the distribution of multiple areas of focal labelling above background (see text). (B) TUNEL assay of 7 μm cryosection (wild type=*Igf2*$^{+m/+p}$ embryo (upper) and littermate *Igf2*$^{+m/-p}$ (lower)). A complex distribution of labelling was observed in both sections. Scale bars: 500 μm in A; 100 μm in B.

(Table 1). In order to determine when the differences in cell number (DNA content) were first established, we examined the relative extent of cell proliferation and cell death in embryos from E8.8 to E11.4, initially timed by plugging (see Materials and Methods for our modification of plug timing). Embryonic cryosections and paraffin embedded sections, from timed matings from 23 litters (68/192 embryos *Igf2*$^{+m/-p}$), were generated and proliferation and cell death examined using BrdU incorporation, Acridine Orange and TUNEL assays. Despite widespread positive staining in wild-type littermates, we could not subjectively detect any differences in BrdU-

Table 1. Body weight, cell number and DNA content in *WT* and *Igf2*$^{+m/-p}$ embryos (~E9 to ~E16) and neonates (P1)

		E9±0.4	E11±0.4	E16±0.5	P1±0.5
Total cell number (×10^5)	Wild type	4.55±0.7	82.0±9.8	ND	ND
	Igf2$^{+m/-p}$	4.2±0.7	62.4±7.9	ND	ND
	Ratio (*n*)	0.92 (28)	0.76 (18)	–	–
Total DNA content (mg)	Wild type	ND	ND	3.0±0.12	3.19±0.14
	Igf2$^{+m/-p}$	ND	ND	2.4±0.11	2.56±0.24
	Ratio (*n*)	–	–	0.79‡ (22)	0.80 (18)
Total weight (g)	Wild type	ND	ND	0.51±0.02	1.17±0.06
	Igf2$^{+m/-p}$	ND	ND	0.31±0.02	0.62±0.06
	Ratio (*n*)	1*	0.75*	0.62‡ (22)	0.53 (18)

Values are mean ± s.e.m. for matched pairs. ND, not determined.
*Data from Baker et al., 1993.
‡Ratio of DNA content and total weight for the total conceptus (E16.5, embryo plus placenta) are 0.85 and 0.69, respectively, compared with Gardner et al., 1999.

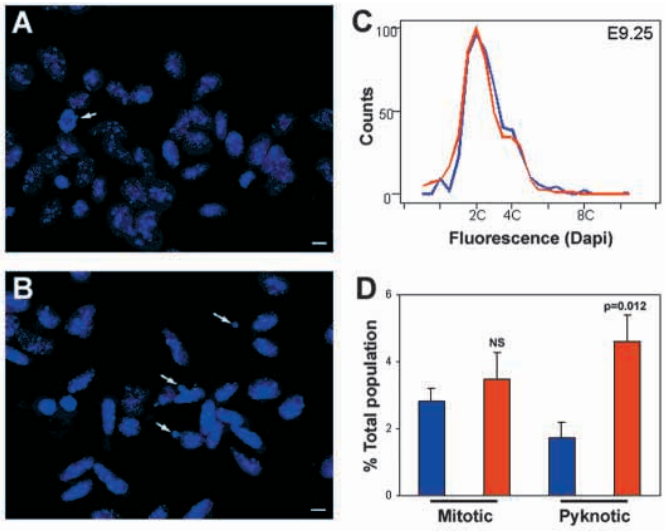

Fig. 2. Analysis of droplet spreads of embryo cell suspensions. (A,B) Droplet spreads of suspensions from whole wild-type (A) and *Igf2*$^{+m/-p}$ (B) embryos stained with DAPI and visualised with fluorescence microscopy. Mitotic figures (arrow in A) and pyknotic cells with less than 2C DNA content (arrows in B) can be identified. (C) Similarity in the distribution of fluorescence emitted per nuclei from litter-matched whole embryo spreads, (wild type (blue) *n*=436 nuclei, *Igf2*$^{+m/-p}$ (red) *n*=499 nuclei). (D) Significantly increased pyknotic cell number in *Igf2*$^{+m/-p}$ cell spreads were observed (**P=0.012 Student's *t*-test, wild type (blue) *n*=2341 nuclei from seven embryos, *Igf2*$^{+m/-p}$ (red) *n*=1277 nuclei from seven embryos). No significant differences (NS) were detected for mitotic cell counts (P=0.47). Scale bars: 10 μm in A,B.

positive cells throughout *Igf2*$^{+m/-p}$ embryos (not shown). Acridine Orange and TUNEL staining revealed similar anatomical sites of cell death through out all embryos. Localisation was particularly prominent at E9.25 during anterior neural fold closure, in the upper forebrain area, rhombencephalon, otics pits, base of the first branchial arch, foregut region, somites and posterior neural folds. After confocal microscopy and TUNEL sections, no subjective increase in cell death was detected between wild-type and *Igf2*$^{+m/-p}$ embryos, either in these regions or in new areas, such as the heart (n=6, Fig. 1). In the maximum projection confocal examples shown in Fig. 1, rotation of the head region of the *Igf2*$^{+m/-p}$ embryo results in an apparent increase in pyknotic cells around the hindbrain region, but examination of sections failed to reveal such differences. However, in these high magnification confocal samples, the size of the *Igf2*$^{+m/-p}$ embryos appeared slightly smaller between E9 and E9.5. This was most obvious when comparing somite size and the dimensions of the first branchial arch, suggesting an overall reduction in embryo size (Fig. 1A and inserts). At this stage such size differences can also occur between littermate wild-type embryos, suggesting normal variation.

Quantification of embryonic cell number in wild type and *Igf2*$^{+m/-p}$ embryos

In order to quantify the cell number increases *in vivo*, we utilised methods which generate single cell suspensions of whole embryos (see Methods) (Heyer et al., 2000; MacAuley et al., 1993). Visualisation of DAPI stained droplet spreads confirmed that most, but not all, cells were separate from each other (Fig. 2A,B). The morphological features of pyknosis and mitosis were identified, and nuclear DNA content quantified using analysis of digital images from unselected fields (Fig. 2C). At E9.25 (timed by plugs), there was a significant increase in the number of pyknotic cells in *Igf2*$^{+m/-p}$ spreads, without a gross difference in DNA content profile, except for a slight increase in sub-diploid (<2C) cells (Fig. 2C,D). Only obvious pyknotic nuclei were counted on spreads, as smaller nuclei and particles could not be confidently identified above background level. When a single particle was located next to several smaller particles, usually one or two, then this was counted as one. Nucleated red cells could be identified as their nuclei had at least a diploid (2C) DNA content, were larger and had a different morphology from pyknotic nuclei which had <2C DNA content (Coles et al., 1993).

After careful dissection of embryos from extra-embryonic membranes, quantification of total embryo cell number was then performed by flow cytometry of whole embryo

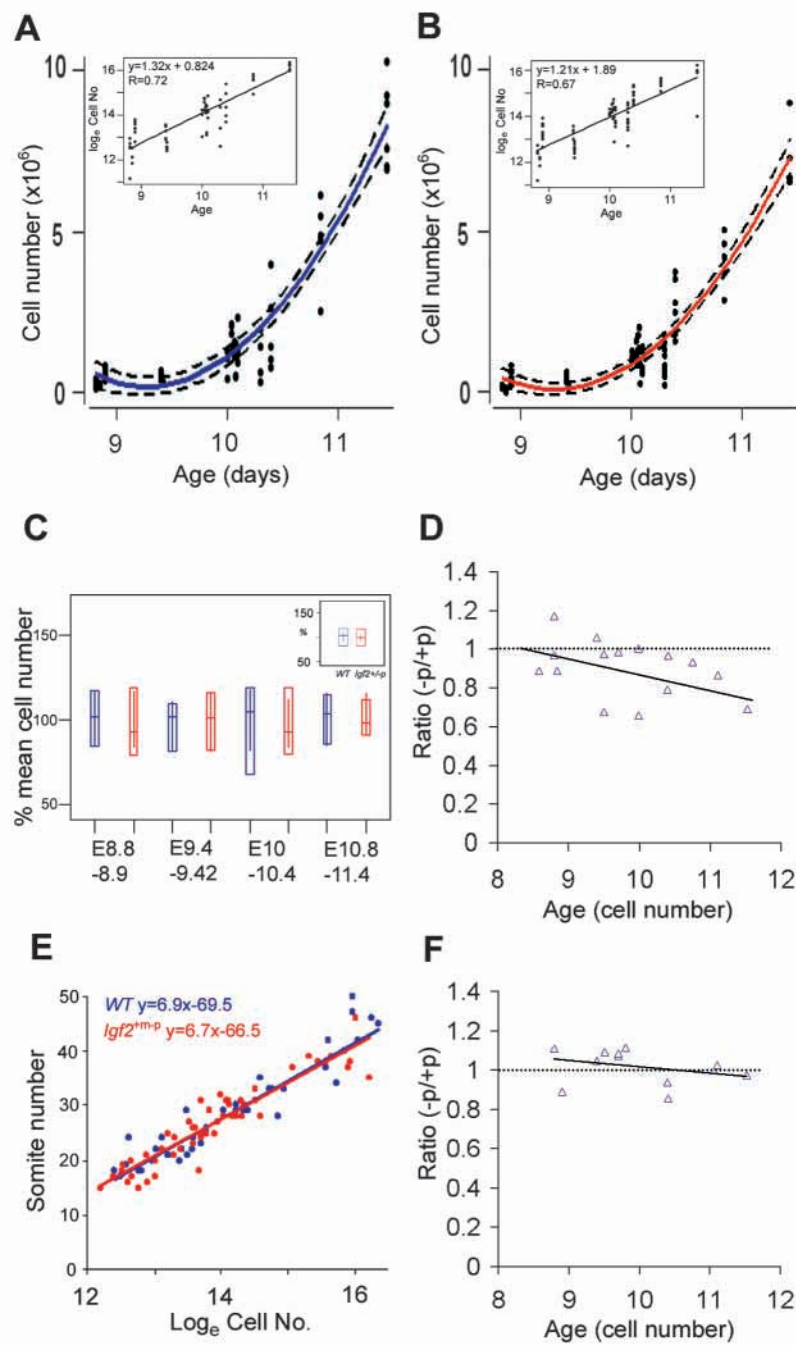

Fig. 3. Flow cytometric analysis of whole embryo cell suspensions. (A,B) Flow cytometric quantification of total cell number (unbroken line) and 95% confidence interval (broken lines) from pooled wild-type (A, n=65) and *Igf2*$^{+m/-p}$ (B, n=84) embryos dated by seminal plugs and using a quadratic line of best fit (Minitab). Inserts show linear plots of log$_e$ cell number versus age (days). (C) Box plots of normalised (100%) cell number (subtracting sub-G1) of each embryo relative to the mean cell number of the respective genotype in each litter (box=interquartile range, vertical line=95% confidence interval, horizontal line=median). Insert shows pooled values. (D) Ratios of mean cell numbers per litter for *Igf2*$^{+m/-p}$ (–p) over wild-type (+p) embryos matched per litter and aged by the mean cell number of wild-type embryos in each litter (blue diamonds, n=15 litters, 140 embryos, P=0.005 at E11, Student's t-test). Line shows linear regression of all data points. (E) Somite number plotted against log$_e$ cell number for wild type (blue, n=65) and *Igf2*$^{+m/-p}$ (red, n=84). (F) Ratios of mean somite numbers and line of best fit for *Igf2*$^{+m/-p}$ (–p) over wild type (+p) embryos matched per litter and aged by the mean cell number of wild-type embryos in each litter (n=10 litters, 124 embryos). Litters with at least two embryos of each genotype were used.

suspensions. This method offered three advantages. First, total cell number was rapidly and reproducibly determined after counting of at least 10,000 cells in suspension from a representative aliquot. Second, sub-G1 particles could be counted as representative of the whole embryo, and finally, quantification of total embryo cell number could be used to age embryos. Controls comparing suspensions before and after fixation with glacial acetic acid/ ethanol showed the same profiles, and sub-G1 cells were not lost during the dissociation of unfixed material (not shown). Furthermore, every propidium iodide-stained suspension was also analysed using peak fluorescence versus total fluorescence to confirm the presence of single cell suspensions (Serna et al., 1998).

Comparison of embryo cell counts at different ages, timed by seminal plugs (see Materials and Methods), showed a rapid increase between E8.8 and E11.4 (Fig. 3A,B). Analysis of pooled data from these embryos showed a plateau in the increase in wild-type and *Igf2*$^{+m/-p}$ embryo cell counts between E8.8 and E9.4 when plotted using a quadratic line of best fit (Fig. 3A,B). Plots of log$_e$ cell number versus age produced linear plots with R values of 0.72 and 0.67 for wild-type and *Igf2*$^{+m/-p}$ embryos, respectively (Fig. 3A,B and inserts). In order to examine the variation between embryos of the same litter with respect to genotype, we normalised each total cell count to the mean cell number value of embryos within each litter (Fig. 3C). Although there was ±20% variation in total cell number between embryos of each litter, this was remarkably similar, irrespective of genotype and age (Fig. 3C, insert). However, such variation highlights the requirement for the analysis of multiple litters within each time range in order to achieve robust statistics.

With respect to the accumulation of cell number, statistically significant differences in total cell number between genotypes, and in cell number subtracting the sub-G1 (<2C) component, were only obtained by E10.8-E11.4 (Table 2). However, closer examination of cell numbers, following subtraction of the sub-G1 component, showed a significant reduction in *Igf2*$^{+m/-p}$ embryo cell number between the ranges E8.8 and E8.9, and E9.4 and E9.42 (P=0.03, Table 2), but were not significant for either wild type or when total counts were compared. Even though examination of mean cell numbers between genotypes was not statistically significant at E9.4-E9.42, presumably because of variation, divergence in cell number appeared to occur by E9.5, when using plugging to date embryos (Table 2).

Embryonic growth has been modelled previously using linear regression and Gompertz equations (Baker et al., 1993; Louvi et al., 1997). Our data can also be modelled by linear regression analysis of an exponential function for the cell number accumulation during the periods between E8.8 and E11.4 (Fig. 3A,B, Table 2). This is not to say that growth is entirely exponential during this period. However, for the purpose of defining the relative timing of embryonic development between litters, we used an equation for the total period E8.8-11.4 (log$_e$ wild-type cell number=1.32x+0.824, where x is the embryonic age) based on wild-type embryo total cell counts (*129/SvJ*) (Fig. 3A and insert). This enabled us to side-step the dependence on plugging alone to time embryonic age, as litters were ranked by determining mean total cell number of wild-type littermates. All subsequent data were then

Table 2. Quantification of cell number in wild type and *Igf2*$^{+m/-p}$ whole embryos aged by plugging

		Total cell number±s.e.m ($\times10^5$)			Total cell number subtracting sub-G1±s.e.m. ($\times10^5$)		
Day	n*	Wild type	*Igf2*$^{+m/-p}$	P‡	Wild type	*Igf2*$^{+m/-p}$	P‡
E8.8-8.9	28	4.8±0.7	4.4±0.6	NS	3.9±0.6	4.0±0.5§	NS
E9.4-9.42	18	4.3±0.6	3.9±0.7	NS	3.1±0.4	2.6±0.3§	NS
E10-10.4	56	18.6±2.1	16.7±1.7	NS	14.6±1.7	13.7±1.3	NS
E10.8-11.4	18	82.0±9.8	62.4±7.9	0.007	62.0±7.5	52.8±7.9	0.004

*Total number of embryos analysed.
‡Student's t-test; NS, not significant.
§Significant reduction between E8.8-8.9 and E9.4-9.42, P=0.03.

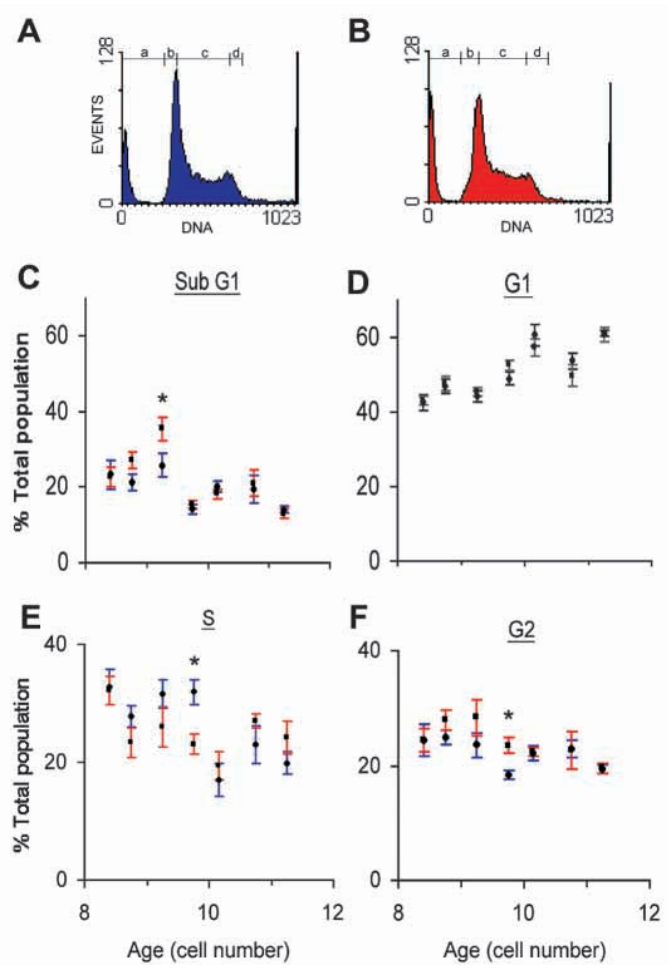

Fig. 4. DNA content and cell cycle parameters of embryo suspensions. (A,B) Representative distribution of DNA content at E9.25 (aged by cell number) of wild-type (A) and *Igf2*$^{+m/-p}$ (B) litter-matched embryos. Gates: Sub-G1=a, G1=2×b, S=c-(b+d) and G2=2×d. (C-F) Quantification of Sub G1(C), G1(D), S (E) and G2 (F) from DNA profiles of litter-matched embryos, as in A,B aged by wild-type embryos at E8.4±0.2 (n=10), E8.8±0.2 (n=26), E9.25±0.25 (n=18), E9.75±0.25 (n=24), E10.15±0.15 (n=22), E10.75±0.25 (n=6) and E11.52±0.25 (n=18). The differences were significant (*) only at E9.25 for sub-G1 (C, P=0.003). E9.75 S-phase (E, P=0.001) and E9.75 G2 (F, P=0.008) (Student's t-test, 95% confidence interval). For D-F, percentages were of total number of viable cells (excluding subG1). Error bars indicate s.e.m.

aged by this method. Extrapolation using a line of best fit of the ratio of *Igf2*$^{+m/-p}$ to wild-type cell number from litter-matched embryos, timed by cell number using our linear regression equation, suggested that the divergence in cell number may have begun by E9.5 (Fig. 3D). Therefore, our data suggest that cell number may be a sensitive predictor of growth, and that differences between wild-type and *Igf2*$^{+m/-p}$ appears to have occurred closer to E9, up to two days before the previously detected differences in whole embryo wet weight (Baker et al., 1993).

Development and cell number in *Igf2*$^{+m/-p}$

Determination of somite number showed that there was a high degree of correlation (wild type and *Igf2*$^{+m/-p}$, R=0.88 for both) between embryonic age, as determined by cell number, and somite number (n=149; Fig. 3E,F). For example, both genotypes had 20 somites at E9.25 and 38 somites at E11. However, the data points were not evenly distributed, and could give the false impression that development of somites proceeds independently of cell number. Ratios of *Igf2*$^{+m/-p}$/wild-type somite number showed that the overall rate of somite increase was the same irrespective of genotype (Fig. 3F). There is an apparent slope in this ratio, and even though statistical analysis of each matched sample showed no significant differences, we cannot exclude a subtle reduction in somite number after E9.5 in *Igf2*$^{+m/-p}$. By contrast, timing of the appearance of otic pits, second branchial arches, apical ectodermal ridges, limb buds and vertebral body number (at E16.5) showed that wild-type and *Igf2*$^{+m/-p}$ embryo developmental timing appeared the same (not shown). Although we have been unable to exclude developmental delay completely, we have to conclude that the overall development of body form appears to proceed independently of cell number throughout this period.

Increased cell death proceeds reduced cell proliferation between E9 and E10 in *Igf2*$^{+m/-p}$

We next quantified cell cycle parameters using flow cytometry of matched littermates. The age of each litter was determined by the mean total cell number of wild-type embryos, using the linear regression equation described. Once all embryos (n=124) were timed by this method, the distribution of the number of embryos against time resulted in random peaks (not shown). We used this distribution to group embryos at times that differed from those used for plugging, e.g. E8.4±0.2, E9.25±0.25, etc. (see Fig. 4). A significant increase in sub-G1-labeled particles in *Igf2*$^{+m/-p}$ embryos was observed at E9.25 compared with wild type (wild type=25.8±2.4% versus *Igf2*$^{+m/-p}$=35.4±3%, n=18, P=0.003, Fig. 4A-C). This observation confirmed pyknotic nuclei counts (Fig. 2D). Sub-G1 counts before and after this time were remarkably similar. After this time, we also detected a significant reduction in the percentage of S-phase cells at E9.75 (wild type=32±2.2% versus *Igf2*$^{+m/-p}$=23±1.7%, n=24, P=0.001, Fig. 4E), and an increase in G2 phase percentage at the same time (wild type=18.3±0.7% versus *Igf2*$^{+m/-p}$=23±1.3%, n=24, P=0.008, Fig. 4F). No significant differences in G1 were detected (wild type=49±1.8% versus *Igf2*$^{+m/-p}$=52±1.3%, n=24, P=0.055, Fig. 4D). In order to exclude the possibility that a component of the sub-G1 population were mitotic chromosomal fragments, we used an antibody to serine 10 α-phosphorylation of histone H3 that is specific for condensed mitotic chromatin. In this case, staining was confined entirely to the mitotic component of the 4C peak and confirmed the lack of chromosomal fragments visible on droplet spreads (Fig. 5). In summary, wild-type embryos showed a discrete increase in cell death and decreased S-phase proportion during this period, and a similar, but exaggerated, trend occurred in *Igf2*$^{+m/-p}$ (Fig. 4).

Although it is likely that sub-G1 counts represent the effects of cell death as described in other stages of embryonic development (Coucouvanis and Martin, 1995; Heyer et al., 2000; MacAuley et al., 1993; Manova et al., 1998), we characterised this further using a caspase-specific assay (Bedner et al., 2000). Using FAM-VAD-FMK, we quantified the proportion of unfixed cells with and without active caspases (1-9) and intact cell membranes (Fig. 6A,B). A small but significant increase in the proportion of cells with active caspases and disrupted membranes occurred in *Igf2*$^{+m/-p}$ at E9.25 (area iii, wild type=23±2.4% versus *Igf2*$^{+m/-p}$= 29±1.8%, n=22, P=0.044; Fig. 6C). No significant differences were detected at E8.5 (wild type=6.75±1.6% versus *Igf2*$^{+m/-p}$= 8.4%±1.3, n=11, P=0.46) and E10.5 (wild type=17.3±4.3% versus *Igf2*$^{+m/-p}$=17.14±6.5%, n=13, P=0.5; Fig. 6C). The increase in cell death assessed by sub-G1 counts in wild-type embryos mirrors the caspase activity detected using this assay (Figs 4C, 6C). At E9.25, significant differences also occurred in the number of cells with disrupted membranes and no increase in caspase activity (area iv, wild type=2.13%±0.4 versus *Igf2*$^{+m/-p}$=3.14%±0.3, n=22, P=0.03, Fig. 6C).

After pulse administration of BrdU, ~25% of cells incorporated label after 1 hour, with <1% also labelled in sub-G1 in wild-type embryos (Fig. 7A). A significant reduction in the proportion of S-phase cells at E9.75 was detected in *Igf2*$^{+m/-p}$ (wild type=25.5±2.1% versus *Igf2*$^{+m/-p}$=22±2.3%, n=16, P=0.006; Fig. 7C) confirming our cytometric profiles, whereas no significant differences were obtained for E8.5 (pooled litters, wild type=42.1% versus *Igf2*$^{+m/-p}$=41.4%, n=8) and E10.5 (wild type=15.8±2.3% versus *Igf2*$^{+m/-p}$=15.5±2.9%, n=13, P=0.95; Fig. 7C). Despite vigorous suspension, up to

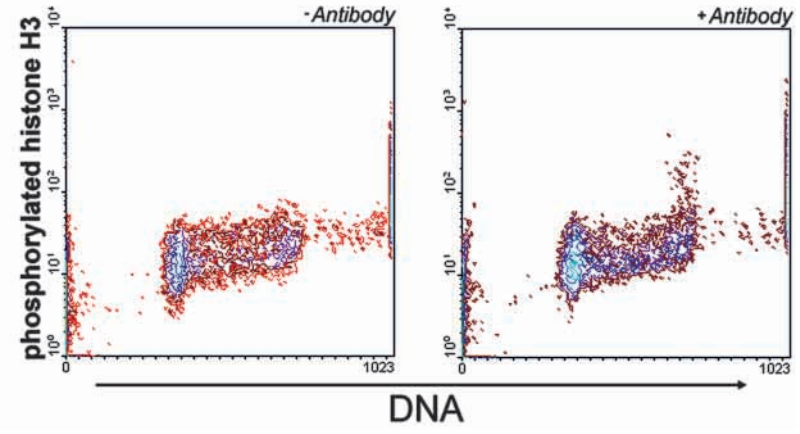

Fig. 5. Cytometric analysis of phosphorylated histone H3 in whole embryo cell suspensions. Right panel shows antibody labelling of mitotic chromatin coinciding with 4C DNA content compared with control (left panel) without primary antibody to serine 10 α-phosphorylation of histone H3.

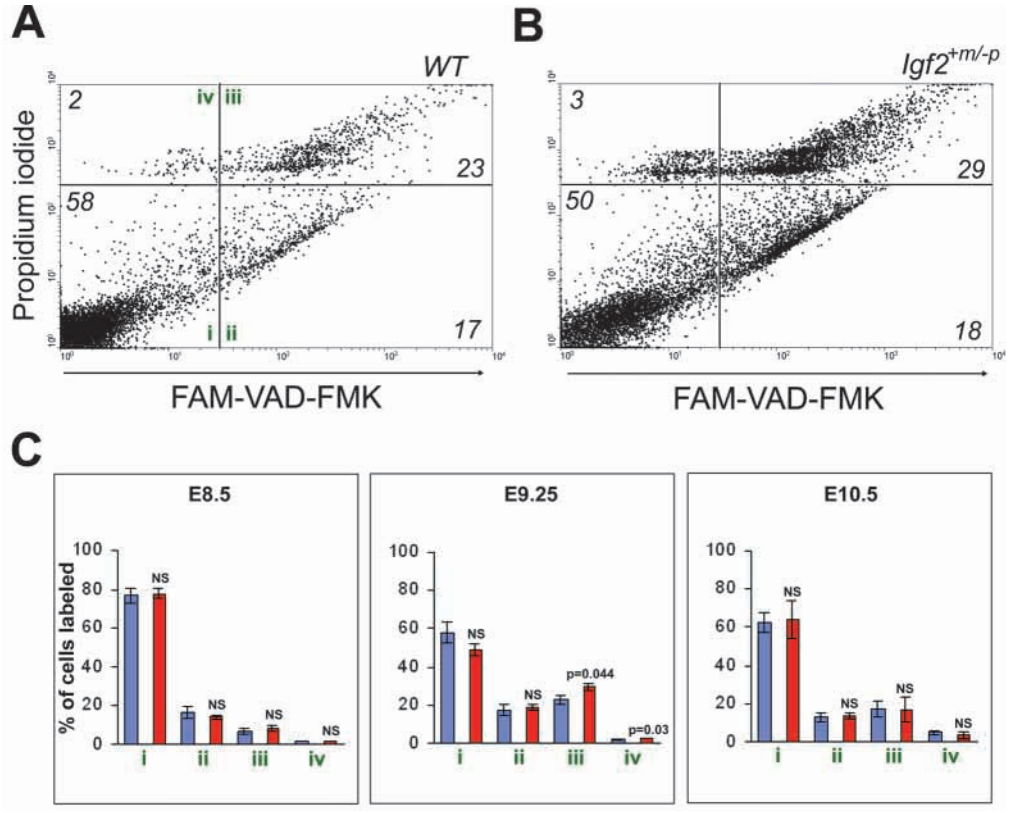

Fig. 6. Analysis of caspase-mediated cell death in unfixed embryo cell suspensions. (A,B) Representative dual colour cytometry from wild type and *Igf2*$^{+m/-p}$ embryos at E9.25 (determined by wild-type embryo cell number) labelled with FAM-VAD-FMK and propidium iodide (PI). FAM-VAD-FMK labels cells with active caspases (1-9) and propidium iodide labels cells with disrupted membranes. FAM-VAD-FMK and PI-positive cells are undergoing apoptosis (area iii), PI-positive cells have disrupted membranes and may be in the late stages of cell death (area iv), FAM-VAD-FMK-positive but PI-negative cells maybe in the earlier commitment phase of cell death (ii) and cells with little caspase activity and intact membranes are viable (i). Numbers indicate mean percentage of whole embryos suspension in each quadrant as in C. (C) Summary of mean±s.e.m. for profiles as in A,B for E8.5± 0.25 (*n*=11), E9.25 (*n*=22) and E10.5± 0.25 (*n*=13) embryos. Significant differences occurred around E9.25, with increased caspase activity and cell permeability in cells from *Igf2*$^{+m/-p}$ embryos (*P*=0.044).

16% and 14% of wild-type and *Igf2*$^{+m/-p}$ cells had greater than diploid (>4C) DNA content, respectively. Analysis of spreads and peak fluorescence during cytometry showed that the majority of these cells were doublets, and that <1% were polyploid (not shown). Doublet cells tended to be in S phase (Fig. 7), which meant that total cell counts from the range ≥2C to ≤4C may underestimate true total numbers.

Pulse incorporation of BrdU at E8.5 in vivo (timing determined by seminal plugs), followed by examination of embryo suspensions 24 hours later, showed that there was a proportion of labelled cells (wild type=6.3±1.3% versus *Igf2*$^{+m/-p}$=8.4±1.4%, *n*=12, *P*=0.049; Fig. 7B,D) that did not appear to have divided during the 24 period. As the subsequent dilution of BrdU staining was heterogenous, indicating that cells within either the wild-type or *Igf*$^{+m/-p}$ embryos had different cell cycle times, this precluded further analysis of the differences between wild type and *Igf2*$^{+m/-p}$.

Of importance, analysis of cell size from cell suspensions of unfixed litter-matched embryos (E9.25) showed no gross difference in cell size peaks (Fig. 8C). We first assessed the high sensitivity of the Coulter method by using red cells suspended in buffers of different osmolarity (Fig. 8A,B). In *Igf2*$^{+m/-p}$ embryos, a small sub-peak was consistently detected that may represent either changes in cell size of a sub-population of cells, altered red blood cells or reflect apoptotic sub-G1 cells. Furthermore, a slight shift to the left occurs in *Igf2*$^{+m/-p}$ profiles (major peak at 7 μm diameter) but this does not appear to be significant. Finally, this analysis cannot exclude a subtle change in cell size in a subpopulation of *Igf2*$^{+m/-p}$ cells and the changes in cell shape that occur when generating cell suspensions.

DISCUSSION

Cell number control during murine embryonic development

Previous estimates of cell number during murine development have relied upon counts from serial sections of fixed tissue usually from specific areas (Coles et al., 1993; Henery et al., 1992; Heyer et al., 2000; Lewis and Rossant, 1982). As a result, cell numbers during gastrulation and organogenesis are not easily quantified. We have used a simple and reliable method of counting cells in embryos (Krasnow et al., 1991; MacAuley et al., 1993; Prober and Edgar, 2000). Cell number accumulation is very rapid between E9 and E11, with an increase in viable embryo cell number from ~400,000 to ~6 million, respectively. Even if a subset of cells divide, many more cells are likely to be generated. For example, if all the cells survived after three cell divisions per day of 50% of the cells at E9, then by E11, 12.8 million cells should have been generated. Thus, a significant (large scale) proportion die in normal embryos during this period. The number of sub-G1 particles and caspase-positive cells reflect this cell death, but we are currently unable to quantify accurately the number and reason for cells dying (Glucksmann, 1951). Despite this, with analysis being partly hampered by the usually high rates of clearance and phagocytosis of apoptotic cells, we estimate that

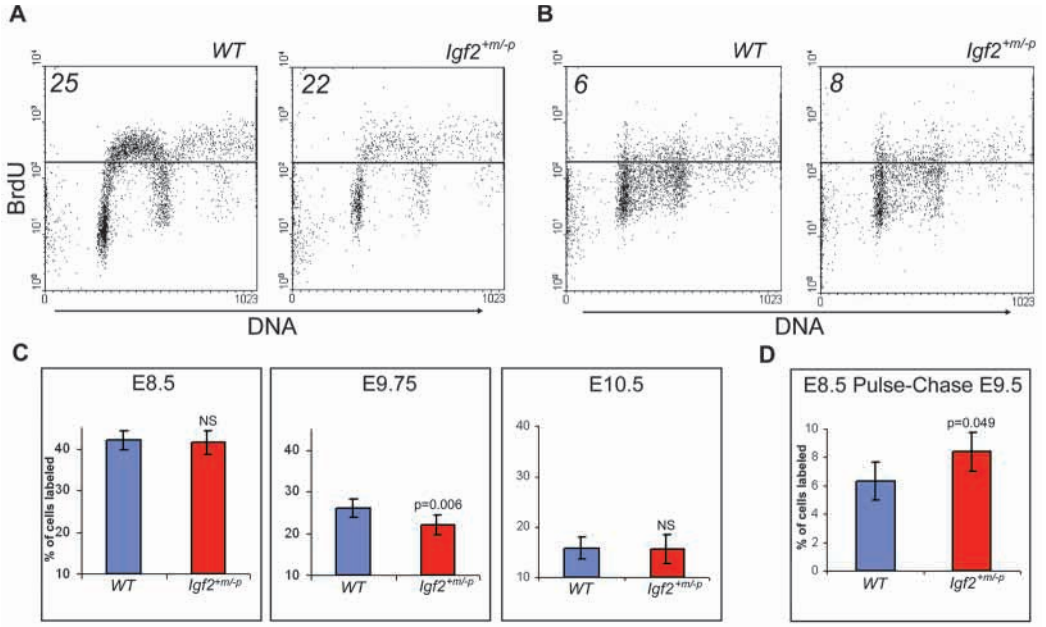

Fig. 7. Cytometric analysis of proliferation determined by BrdU incorporation. (A) Pulse BrdU followed by cytometry of whole embryo suspensions after 1 hour. Typical profiles for wild-type (left panel) and *Igf2*$^{+m/-p}$ (right panel) litter-matched embryos aged at E9.75 by cell number. Numbers indicate mean cell number above the horizontal line as a percentage of whole embryos (n=16). (B) Pulse-chase BrdU followed by cytometry of whole embryo suspensions after 24 hours in vivo. Typical profiles for wild-type (left panel) and *Igf2*$^{+m/-p}$ (right panel) of litter-matched embryos injected at E8.5 and dissected at E9.5 (plugging). The cells above the horizontal line were labelled as after a single BrdU pulse. Numbers indicate mean cell number above the horizontal line as a percentage of whole embryos (n=12). (C) Mean±s.e.m. of percentage of pulse BrdU incorporation as in A at E8.5 (n=8), E9.75 (n=16) and E10.5 (n=13). The only significant differences occurred at E9.75 (P=0.006). (D) Means±s.e.m. of percentage of pulse (E8.5) chase (to E9.5) BrdU incorporation as in B. Fewer cells divided in *Igf2*$^{+m/-p}$, as significantly more retained label as if pulsed at 1 hour (n=12, litter-matched samples).

around 20% of live embryo cells are poised for cell death, as judged by caspase activity and membrane permeability (Fig. 6; Coles et al., 1993; Rassoulzadegan et al., 2000; Wood et al., 2000).

Previous work suggests that there are at least two discrete periods of embryonic growth control that involve modification of cell cycle time and cell death. For example, the period of IGF2 effect we describe coincides with a period of catch up growth (E8-E11) associated with half embryos generated by destruction of one blastomere (Lewis and Rossant, 1982; Rands, 1986b). Furthermore, the growth of organ systems at this time, the first being the heart and major vessels, depends on the local control of cell survival (Shioi et al., 2000). In addition, extensive caspase-dependent cell death occurs during neural tube closure (Weil et al., 1997). An earlier growth control time period (~E6-E7) is associated with the reduction in cell number after early stage embryo aggregation and coincides with early gastrulation (Buehr and McLaren, 1974; Lewis and Rossant, 1982; Rands, 1986a). Here, the distribution of growth factor-dependent cell death is commonly higher in the distal anterior region after the onset of mesoderm formation, and is rarely detected in extra-embryonic ectoderm (Manova et al., 1998). At least 5% of the embryonic cells appear apoptotic between E5.5-E6.5, which can rise to 40% after low dose irradiation (Heyer et al., 2000). The remarkably similar growth of tetraploid embryos to E11, except for the growth of the forebrain, suggests that the embryos appear to control cell mass, perhaps via control of morphogen gradients, rather than absolute cell numbers during this period of development (Henery et al., 1992). Embryo cell number at E7.5 has been estimated to be 16,000 with cell cycle times of ~7 hours in the endoderm and mesoderm (Henery et

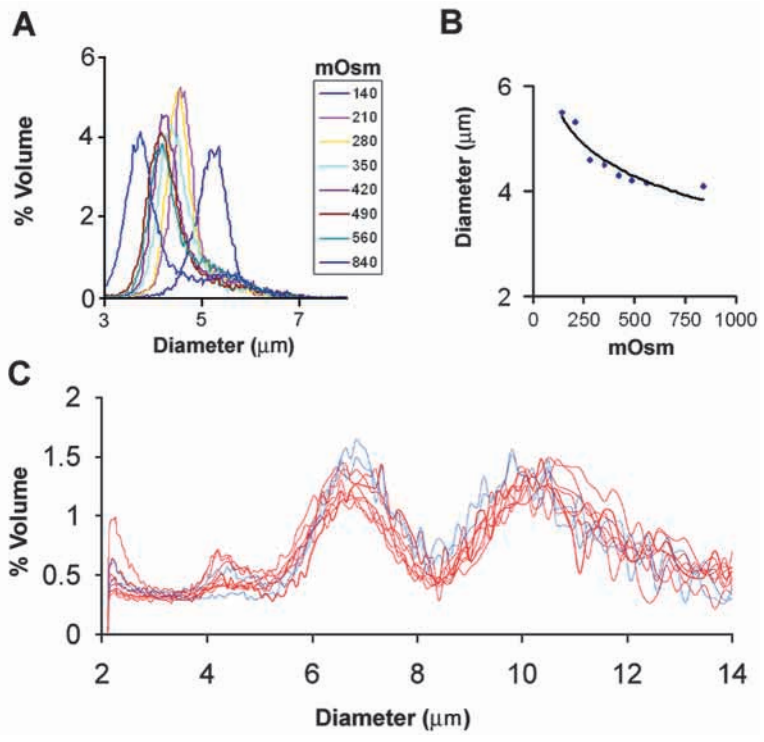

Fig. 8. Cell size analysis of unfixed cells in suspension. (A) Red blood cell (mouse) size distribution profiles following incubation in buffers of different osmolarity (insert) using a Coulter multi-sizer. (B) Red blood cell changes in cell size with osmolarity, from A. (C) Multiple cell diameter profiles from unfixed whole wild-type (blue, n=5) and *Igf2*$^{+m/-p}$ (red, n=6) litter-matched embryos, aged E9.5 using cell number of a fixed wild-type embryo.

al., 1992; Snow, 1976). The notable exception appears to be the cells of the primitive streak, which express *N-myc* but not *Igf2*, where cell cycle times appear to be approximately 3-3.5 hours when estimated using stathmokinetic analysis (Downs et al., 1989; MacAuley et al., 1993). Extrapolating from the accumulation of cell number, we estimate that cell doubling time would be ~10 hours between E8.8 and E11.4, which suggests that the principal period of IGF2 effect occurs over a population average of two to four cell cycles (E9-E10). Once cells are lost, any compensatory mechanisms do not appear to rescue organism size after the E9.25 period (catch up growth, Table 1).

Elegant genetic studies in *Drosophila* have confirmed observations in yeast that control of cell growth can override mechanisms of cell cycle progression (Johnston et al., 1999; Neufeld et al., 1998; Prober and Edgar, 2000). At least in the *Drosophila* wing, co-ordination of both G1 (proliferation) and G2 (growth) appears to be via E2F-mediated expression of both cyclin E and Cdc25/string, respectively (Neufeld et al., 1998). As with E2F, the effect of Myc also appears to be on cyclin E post-transcriptional control of G1/S duration, but also on growth, as cells that overexpress Myc are larger, whereas cells that over-express cyclin E are smaller (Iritani and Eisenman, 1999; Johnston et al., 1999). Unlike E2F, the effect of Myc on growth is not thought to be mediated by Cdc25/string (Johnston et al., 1999). Insulin, related insulin-like ligands, PI3 kinase, Akt/PKB and PTEN phosphatase also modulate cell growth in *Drosophila* (Bohni et al., 1999; Brogiolo et al., 2001; Goberdhan et al., 1999; Weinkove et al., 1999). In the case of cell autonomous growth activity via the *Drosophila* insulin receptor, the effect may be mediated through two pathways. First, PI3K effects on cell size mediated by Akt (PKB) inactivation of translational repression by 4E-BPI, and second, IRS/Grb2 linked effects to the Ras/MAPK kinase pathway to control cell proliferation (Brogiolo et al., 2001; Gingras et al., 1998; Yang and Kastan, 2000).

There are several explanations for the differences in growth between wild-type and $Igf2^{+m/-p}$ embryos: first, each cell could have undergone one less cell cycle; second, a complete generation of newly divided cells could have died; third, a timing mechanism could lead to early withdrawal from the cell cycle; fourth, cell number may the same, but cell size differs; and finally, a combination of the above. In our experiments, it appears that the limited supply of IGF2 has consequences on cell survival and division. The effect may arise because of either limited ligand alone, or because of concomitant increased expression of growth signals such as *myc* or *p53*, unmasking the lack of IGF2-mediated cell survival. A trivial explanation may also relate to lack of nutrient and oxygen supply. However, in our view, the magnitude and reproducibility of the growth defect suggests that the effect is developmentally programmed. Furthermore, although the differences we detect in cell proliferation and cell death are subtle between E9 and E10, and we cannot exclude effects either side of this time period, they coincide with the irreversible and significant differences in cell number throughout the rest of gestation and adult life. As it is likely that limiting ligand supply will simultaneously modify multiple pathways depending on cell type, it is not surprising that we can detect no differences in cell size (Fig. 8).

Does insulin-like growth factor 2 control adult size by modifying cell number during a discrete period of post-implantation development?

The proportional growth of a mouse is thought to be controlled during two growth periods, one during development (IGF2), the other relating to the prolonged growth effects after this time (IGF1; Baker et al., 1993; Lupu et al., 2001). Our data now eludes to the possibility that IGF2-mediated control of whole organism growth may occur during a developmental period of only a few cell cycles. However, the questions remain as to whether this is the sole period of IGF2 action, and whether the extent and duration of IGF2 supply controls size differences between species.

Analysis of our data with that of Baker et al. and Gardner et al. suggests that the reduction in whole organism weight of $Igf2^{+m/-p}$ (38-47% E16 and P1, Table 1) is more extensive than the reduction in DNA content or cell number (20-21%), at least between E11.0 and P1 (Table 1; Baker et al., 1993; Gardner et al., 1999). The apparent reduction in weight alone at ~E11 to only 75% of wild-type littermates, which then reduces further to ~60% by E16, could be viewed as evidence that argues against there being a single discrete period of IGF2 control of cell number (Baker et al., 1993). The results of inner cell mass and trophectoderm exchange experiments suggest that such a discrepancy may be due to the relative lack of extracellular fluid accumulation in $Igf2^{+m/-p}$ conceptuses, when compared with differences in DNA content at E16 (Gardner et al., 1999). Here, a greater component of total weight in the wild-type conceptus was accounted for by fluid content, e.g. that associated with ECM, compared with $Igf2^{+m/-p}$, without changes in DNA content (Gardner et al., 1999). Increased IGF2 supply in development can result in overgrowth, e.g. either after disruption of *Igf2r* (+130%) or biallelic *Igf2* expression (+130%; Eggenschwiler et al., 1997; Lau et al., 1994; Ludwig et al., 1996). In the former case, oedema occurs with overgrowth of the placenta (Baker et al., 1993; Louvi et al., 1997). In the latter case, oedema does not occur, even though placental growth is similar to that in $Igf2r^{-m/+p}$ (Eggenschwiler et al., 1997). In neither case is cell number or DNA content known. The proportional overgrowth that occurs during *H19* disruption can be rescued to wild-type size by $Igf2^{+m/-p}$ (Leighton et al., 1995). Even though combination of $Igf^{+m/-p}$ and $Igf2r^{-m/+p}$ results in rescue of viability, the animals remain smaller and have the same growth phenotype as $Igf^{+m/-p}$ (60% of wild type) (Ludwig et al., 1996). A combination of $Igf2r^{-m/+p}$ and disruption of *H19* results in further overgrowth with phenotypic features that are consistent with those seen in Beckwith Wiedemann syndrome (Eggenschwiler et al., 1997). Overall, these experiments further suggest that IGF2 controls cell number, presumably between E9 and E10, but can also result in fluid accumulation after this time period. Interestingly, using Western blots on embryonic extracts, tissue levels of IGF2 at E12.5 are similar in both $Igf2r^{-m/+p}$ and disruption of *H19*, at least twofold higher than wild type, but fall to 1.4 in the former by E13.5 and are at least sevenfold higher when genotypes are combined (Eggenschwiler et al., 1997; Ludwig et al., 1996). However, the correlation between IGF2 supply and cell number has yet to be established. After E9-E10, IGF2 supply is limited by the sequestration function of IGF2/M6P receptor present at similar sites (Lee et al., 1990; Senior et al., 1990; Wutz et al., 2001). Furthermore, the recovery of cell

survival and proliferation to wild-type levels after this period may also arise because of rescue by later production of IGF1 (Baker et al., 1996; Baker et al., 1993).

We do not know either the cause of the relative increase in cell death or decreased S-phase (E9.25-E9.75) that is exaggerated in *Igf2*$^{+m/-p}$ embryos, and whether there is a sensing organ that monitors growth and controls IGF2 supply (Snow et al., 1981). IGF2 supply may modify a crucial population of cells, each either with an autonomous growth program, or an ability to control cell numbers of determined cells situated in close proximity (de Bruijn et al., 2000; Gandarillas and Watt, 1997; Gao et al., 1997; Gurdon, 1988; Johnston et al., 1999; Slack, 2000). Functionally, the period of IGF2 effect on embryo cell number may demarcate development into two stages: an initial phase that is predominantly associated with the development of form, perhaps when the number of determined stem (source) cells are genetically regulated, followed by a second growth phase, when the limits to mammalian organ size are established.

We thank Ted Evans, Chris Graham and Richard Gardner for early discussion, and Louis Mahadevan for anti-H3 antibody, and the CRC and BBSRC for support.

REFERENCES

Abrams, J. M., White, K., Fessler, L. I. and Steller, H. (1993). Programmed cell death during Drosophila embryogenesis. *Development* **117**, 29-43.

Araki, E., Lipes, M. A., Patti, M. E., Bruning, J. C., Haag, B., 3rd, Johnson, R. S. and Kahn, C. R. (1994). Alternative pathway of insulin signalling in mice with targeted disruption of the IRS-1 gene. *Nature* **372**, 186-190.

Baker, J., Hardy, M. P., Zhou, J., Bondy, C., Lupu, F., Bellve, A. R. and Efstratiadis, A. (1996). Effects of an Igf1 gene null mutation on mouse reproduction. *Mol. Endocrinol.* **10**, 903-918.

Baker, J., Liu, J. P., Robertson, E. J. and Efstratiadis, A. (1993). Role of insulin-like growth factors in embryonic and postnatal growth. *Cell* **75**, 73-82.

Bedner, E., Smolewski, P., Amstad, P. and Darzynkiewicz, Z. (2000). Activation of caspases measured in situ by binding of fluorochrome-labeled inhibitors of caspases (FLICA): correlation with DNA fragmentation. *Exp. Cell Res.* **259**, 308-313.

Bi, L., Okabe, I., Bernard, D. J., Wynshaw Boris, A. and Nussbaum, R. L. (1999). Proliferative defect and embryonic lethality in mice homozygous for a deletion in the p110alpha subunit of phosphoinositide 3-kinase. *J. Biol. Chem.* **274**, 10963-10968.

Bohni, R., Riesgo-Escovar, J., Oldham, S., Brogiolo, W., Stocker, H., Andruss, B. F., Beckingham, K. and Hafen, E. (1999). Autonomous control of cell and organ size by CHICO, a Drosophila homolog of vertebrate IRS1-4. *Cell* **97**, 865-875.

Brogiolo, W., Stocker, H., Ikeya, T., Rintelen, F., Fernandez, R. and Hafen, E. (2001). An evolutionary conserved function of the Drosophila insulin receptor and insulin-like peptides in growth control. *Curr. Biol.* **11**, 213-221.

Buehr, M. and McLaren, A. (1974). Size regulation in chimaeric mouse embryos. *J. Embryol. Exp. Morphol.* **31**, 229-234.

Christofori, G., Naik, P. and Hanahan, D. (1995). Deregulation of both imprinted and expressed alleles of the insulin-like growth factor 2 gene during beta-cell tumorigenesis. *Nat. Genet.* **10**, 196-201.

Coles, H. S. R., Burne, J. F. and Raff, M. C. (1993). Large-scale normal cell death in the developing rat kidney and its reduction by epidermal growth factor. *Development* **118**, 777-784.

Conlon, I. and Raff, M. (1999). Size control in animal development. *Cell* **96**, 235-244.

Coucouvanis, E. and Martin, G. R. (1995). Signals for death and survival: a two-step mechanism for cavitation in the vertebrate embryo. *Cell* **83**, 279-287.

Da Costa, T. H., Williamson, D. H., Ward, A., Bates, P., Fisher, R., Richardson, L., Hill, D. J., Robinson, I. C. and Graham, C. F. (1994). High plasma insulin-like growth factor-II and low lipid content in transgenic mice: measurements of lipid metabolism. *J. Endocrinol.* **143**, 433-439.

Datta, S. R., Dudek, H., Tao, X., Masters, S., Fu, H., Gotoh, Y. and Greenberg, M. E. (1997). Akt phosphorylation of BAD couples survival signals to the cell-intrinsic death machinery. *Cell* **91**, 231-241.

de Bruijn, M. E. T. R., Speck, N. A., Peeters, M. C. E. and Dzierzak, E. (2000). Definitive hematopoetic stem cells first develop within the major arterial regions of the mouse embryo. *EMBO J.* **19**, 2465-2474.

DeChiara, T. M., Efstratiadis, A. and Robertson, E. J. (1990). A growth-deficiency phenotype in heterozygous mice carrying an insulin-like growth factor II gene disrupted by targeting. *Nature* **345**, 78-80.

DeChiara, T. M., Robertson, E. J. and Efstratiadis, A. (1991). Parental imprinting of the mouse insulin-like growth factor II gene. *Cell* **64**, 849-859.

Downs, K. M., Martin, G. R. and Bishop, J. M. (1989). Contrasting patterns of myc and N-myc expression during gastrulation of the mouse embryo. *Genes Dev.* **6**, 860-869.

Downward, J. (1998). Mechanisms and consequences of activation of protein kinase B/Akt. *Curr. Opin. Cell Biol.* **10**, 262-267.

Efstratiadis, A. (1998). Genetics of mouse growth. *Int. J. Dev. Biol.* **42**, 955-976.

Eggenschwiler, J., Ludwig, T., Fisher, P., Leighton, P. A., Tilghman, S. M. and Efstratiadis, A. (1997). Mouse mutant embryos overexpressing IGF-II exhibit phenotypic features of the Beckwith-Wiedemann and Simpson-Golabi-Behmel syndromes. *Genes Dev.* **11**, 3128-3142.

Gandarillas, A. and Watt, F. M. (1997). c-myc promotes differentiation of human epidermal stem cells. *Genes Dev.* **11**, 2869-2882.

Gao, F.-B., Durand, B. and Raff, M. (1997). Oligodendrocyte precursor cells count time but not cell divisions before differentiation. *Curr. Biol.* **7**, 152-155.

Gardner, R. L., Squire, S., Zaina, S., Hills, S. and Graham, C. F. (1999). Insulin-like growth factor 2 regulation of conceptus composition: effects of the trophectoderm and inner cell mass genotypes in the mouse. *Biol. Reprod.* **60**, 190-195.

Gingras, A. C., Kennedy, S. G., O'Leary, M. A., Sonenberg, N. and Hay, N. (1998). 4E-BP1, a repressor of mRNA translation, is phosphorylated and inactivated by the Akt(PKB) signaling pathway. *Genes Dev.* **12**, 502-513.

Glucksmann, A. (1951). Cell deaths in normal vertebrate ontogeny. *Biol. Rev.* **26**, 59-86.

Goberdhan, D. C., Paricio, N., Goodman, E. C., Mlodzik, M. and Wilson, C. (1999). Drosphila tumor suppressor PTEN controls cell size and number by antagonizing the Chico/PI3-kinase signaling pathway. *Genes Dev.* **13**, 3244-3258.

Grandjean, V., Smith, J., Scofield, P. N. and Ferguson-Smith, A. C. (2000). Increased IGF-II protein affects p57kip2 expression in vivo and in vitro: implications for Beckwith-Weidemann syndrome. *Proc. Natl. Acad. Sci. USA* **97**, 5279-5284.

Gurdon, J. B. (1988). A community effect in animal development. *Nature* **336**, 772-774.

Hassan, A. B. and Howell, J. A. (2000). Insulin-like growth factor II (IGF-II) supply modifies growth of intestinal adenoma in Apc Min/+ mice. *Cancer Res.* **60**, 1070-1076.

Henery, C. C., Bard, J. B. L. and Kaufman, M. H. (1992). Tetraploidy in mice, embryonic cell number, and the grain of the developmental map. *Dev. Biol.* **152**, 233-241.

Heyer, B. S., MacAuley, A., Behrendtsen, O. and Werb, Z. (2000). Hypersensitivity to DNA damage leads to increased apoptosis during early mouse development. *Genes Dev.* **14**, 2072-2084.

Iritani, B. M. and Eisenman, R. N. (1999). c-myc enhances protein synthesis and cell size during B lymphocyte development. *Proc. Natl. Acad. Sci. USA* **96**, 13180-13185.

Johnston, L. A., Prober, D. A., Edgar, B. A., Eisenman, R. N. and Gallant, P. (1999). Drosophila myc regulates cellular growth during development. *Cell* **98**, 779-790.

Krasnow, M. A., Cumberledge, S., Manning, G., Herzenberg, L. A. and Nolan, G. P. (1991). Whole animal cell sorting of Drosophila embryos. *Science* **251**, 81-85.

Labarca, C. and Paigen, K. (1980). A simple, rapid, and sensitive DNA assay procedure. *Anal. Biochem.* **102**, 344-352.

Lau, M. M., Stewart, C. E., Liu, Z., Bhatt, H., Rotwein, P. and Stewart, C. L. (1994). Loss of the imprinted IGF2/cation-independent mannose 6-phosphate receptor results in fetal overgrowth and perinatal lethality. *Genes Dev.* **8**, 2953-2963.

Lee, J. E., Pintar, J. and Efstratiadis, A. (1990). Pattern of the insulin-like growth factor-II gene expression during early mouse embryogenesis. *Development* **110**, 151-159.

Leighton, P. A., Ingram, R. S., Eggenschwiler, J., Efstratiadis, A. and Tilghman, S. M. (1995). Disruption of imprinting caused by deletion of the H19 gene region in mice. *Nature* **375**, 34-39.

Lewis, N. E. and Rossant, J. (1982). Mechanism of size regulation in mouse embryo aggregates. *J. Embryol. Exp. Morphol.* **72**, 169-181.

Liu, J. P., Baker, J., Perkins, A. S., Robertson, E. J. and Efstratiadis, A. (1993). Mice carrying null mutations of the genes encoding insulin-like growth factor I (Igf-1) and type 1 IGF receptor (Igf1r). *Cell* **75**, 59-72.

Lopez, M. F., Dikkes, P., Zurakowski, D. and Villa-Komaroff, L. (1996). Insulin-like growth factor II affects the appearance and glycogen content of glycogen cells in the murine placenta. *Endocrinology* **137**, 2100-2108.

Louvi, A., Accili, D. and Efstratiadis, A. (1997). Growth-promoting interaction of IGF-II with the insulin receptor during mouse embryonic development. *Dev. Biol.* **189**, 33-48.

Ludwig, T., Eggenschwiler, J., Fisher, P., D'Ercole, A. J., Davenport, M. L. and Efstratiadis, A. (1996). Mouse mutants lacking the type 2 IGF receptor (IGF2R) are rescued from perinatal lethality in Igf2 and Igf1r null backgrounds. *Dev. Biol.* **177**, 517-535.

Lupu, F., Terwilliger, J. D., Lee, K., Segre, G. V. and Efstratiadis, A. (2001). Roles of growth hormone and insulin-like growth factor I in mouse postnatal growth. *Dev. Biol.* **229**, 141-162.

MacAuley, A., Werb, Z. and Mirkes, P. E. (1993). Characterization of the unusally rapid cell cycles during rat gastrulation. *Development* **117**, 873-883.

Manova, K., Tomihara-Newberger, C., Wang, S., Godelman, A., Kalantry, S., Witty-Blease, K., De Leon, V., Chen, W. S., Lacy, E. and Bachvarova, R. F. (1998). Apoptosis in mouse embryos: elevated levels in pregastrulae and in the distal anterior region of gastrulae of normal and mutant mice. *Dev. Dyn.* **213**, 293-308.

Morali, O. G., Jouneau, A., McLaughlin, J., Theiry, J. P. and Larue, L. (2000). IGF-II promotes mesoderm formation. *Dev. Biol.* **227**, 133-145.

Neufeld, T. P., de al Cruz, A., Johnston, L. A. and Edgar, B. A. (1998). Co-ordination of growth and cell division in the Drosophila wing. *Cell* **93**, 1183-1193.

Nielson, J., Christianson, J., Lykke-Anderson, J., Johnsen, A. H., Wewer, U. M. and Nielsen, F. C. (1999). A family of insulin-like growth factor II mRNA binding proteins represses translation in late development. *Mol. Cell. Biol.* **19**, 1262-1270.

Prober, D. A. and Edgar, B. A. (2000). Ras1 promotes cellular growth in the Drosophila wing. *Cell* **100**, 435-446.

Rands, G. F. (1986a). Size regulation in the mouse embryo I. The development of quadruple aggregates. *J. Embryol. Exp. Morphol.* **94**, 139-148.

Rands, G. F. (1986b). Size regulation in the mouse embryo II. The development of half embryos. *J. Embryol. Exp. Morphol.* **98**, 209-217.

Rassoulzadegan, M., Rosen, B. S., Gillot, I. and Cuzin, F. (2000). Phagocytosis reveals a reversible differentiated state early in the development of the mouse embryo. *EMBO J.* **13**, 3295-3303.

Senior, P. V., Byrne, S., Brammer, W. J. and Beck, F. (1990). Expression of the IGF-II/mannose 6-phosphate receptor mRNA and protein in the developing rat. *Development* **109**, 67-73.

Serna, J., Pimentel, B. and de la Rosa, E. (1998). Flow cytometric analysis of whole organs and embryos. *Curr. Top. Dev. Biol.* **36**, 211-222.

Shioi, T., Kang, P. M., Douglas, P. S., Hampe, J., Yballe, C. M., Lawitts, J., Cantley, L. C. and Izumo, S. (2000). The conserved phosphoinositide 3-kinase pathway determines heart size in mice. *EMBO J.* **19**, 2537-2548.

Sicinski, P., Donaher, J. L., Parker, S. B., Li, T., Fazeli, A., Gardner, H., Haslam, S. Z., Bronson, R. T., Elledge, S. J. and Weinberg, R. A. (1995). Cyclin D1 provides a link between development and oncogenesis in the retina and breast. *Cell* **82**, 621-630.

Slack, J. M. (2000). Stem cells in epithelial tissues. *Science* **287**, 1431-1433.

Snow, M. H. L. (1976). Embryo growth during the immediate postimplantation period. In *Embryogenesis in Mammals* (*CIBA Found. Symp.*) (ed. K. Elliott and M. O'Connor). Vol. 40, pp. 53-70. Amsterdam, Oxford, New York: Elsevier.

Snow, M. H. L., Tam, P. P. L. and McLaren, A. (1981). On the control and regulation of size and morphogenesis in mammalian embryos. In *Levels of Genetic Control in Development* (ed. S. Subtekny and U. K. Abbott), pp. 201-217. New York: Alan Liss.

Srivastava, M., Hsieh, S., Williams-Simons, L., Huang, S.-P. and Pfeifer, K. (2000). H19 and Igf2 monoallelic expression is regulated in two distinct ways by a shared cis acting regulatory region upstream of H19. *Genes Dev.* **14**, 1186-1195.

Sun, F. L., Dean, W. L., Kelsey, G., Allen, N. D. and Reik, W. (1997). Transactivation of Igf2 in a mouse model of Beckwith-Wiedemann syndrome. *Nature* **389**, 809-815.

Tilghman, S. M. (1999). The sins of the fathers and mothers: genomic imprinting in mammalian development. *Cell* **96**, 185-193.

Tough, D. F. and Sprent, J. (1994). Turnover of naive- and memory-phenotype T cells. *J. Exp. Med.* **179**, 1127-1135.

Van der Velden, A. W., Destree, O. H. J., Voorma, H. O. and Thomas, A. A. (2000). Controlled translation initiation on Insulin-like growth factor leader 1 during Xenopus laevis embryogenesis. *Int. Rev. Dev. Biol.* **44**, 843-850.

Weil, M., Jacobson, M. D. and Raff, M. C. (1997). Programmed cell death required for neural tube closure? *Curr. Biol.* **7**, 281-284.

Weinkove, D., Neufeld, T. P., Twardzik, T., Waterfield, M. D. and Leevers, S. J. (1999). Regulation of imaginal disc cell size, cell number and organ size by Drosophila class 1(A) phosphoinositide 3-kinase and its adapter. *Curr. Biol.* **9**, 1019-1029.

Wood, W., Turmaine, M., Weber, R., Camp, V., Maki, R. A., McKercher, S. R. and Martin, P. (2000). Mesenchymal cells engulf and clear apoptotic footplate cells in macrophagesless PU.1 null mouse embryos. *Development* **127**, 5245-5252.

Wutz, A., Theussi, H. C., Dausman, J., Jaenisch, R., Barlow, D. P. and Wagner, E. F. (2001). Non-imprinted Igf2r expression decreases growth and rescues the Tme mutation in mice. *Development* **128**, 1881-1887.

Yang, D. Q. and Kastan, M. B. (2000). Participation of ATM in insulin signalling through phosphorylation of eIF-4E-binding protein 1. *Nat. Cell Biol.* **2**, 893-898.

Young, L. E., Fernandes, K., McVoy, T. G., Butterwith, S. C., Gutierrez, C. G., Carolan, C., Broadbent, P. J., Robinson, J. J., Wilmut, I. and Sinclair, K. D. (2001). Epigenetic change in IGF2R is associated with fetal overgrowth after sheep embryo culture. *Nat. Genet.* **27**, 153-154.

Zaina, S. and Squire, S. (1998). The soluble type 2 insulin-like growth factor (IGF-II) receptor reduces organ size by IGF-II-mediated and IGF-II-independent mechanisms. *J. Biol. Chem.* **273**, 28610-28616.